

# Integration of a Spectral Domain Optical Coherence Tomography System into a Surgical Microscope for Intraoperative Imaging

Justis P. Ehlers,<sup>1,2</sup> Yuankai K. Tao,<sup>3</sup> Sina Farsiu,<sup>1,3</sup> Ramiro Maldonado,<sup>1</sup> Joseph A. Izatt,<sup>1,3</sup> and Cynthia A. Toth<sup>1,3</sup>

**PURPOSE.** To demonstrate an operating microscope-mounted spectral domain optical coherence tomography (MMOCT) system for human retinal and model surgery imaging.

**METHODS.** A prototype MMOCT system was developed to interface directly with an ophthalmic surgical microscope, to allow SDOCT imaging during surgical viewing. Nonoperative MMOCT imaging was performed in an Institutional Review Board-approved protocol in four healthy volunteers. The effect of surgical instrument materials on MMOCT imaging was evaluated while performing retinal surface, intraretinal, and subretinal maneuvers in cadaveric porcine eyes. The instruments included forceps, metallic and polyamide subretinal needles, and soft silicone-tipped instruments, with and without diamond dusting.

**RESULTS.** High-resolution images of the human retina were successfully obtained with the MMOCT system. The optical properties of surgical instruments affected the visualization of the instrument and the underlying retina. Metallic instruments (e.g., forceps and needles) showed high reflectivity with total shadowing below the instrument. Polyamide material had a moderate reflectivity with subtotal shadowing. Silicone instrumentation showed moderate reflectivity with minimal shadowing. Summed voxel projection MMOCT images provided clear visualization of the instruments, whereas the B-scans from the volume revealed details of the interactions between the tissues and the instrumentation (e.g., subretinal space cannulation, retinal elevation, or retinal holes).

**CONCLUSIONS.** High-quality retinal imaging is feasible with an MMOCT system. Intraoperative imaging with model eyes provides high-resolution depth information including visualization of the instrument and intraoperative tissue manipulation. This study demonstrates a key component of an interactive platform that could provide enhanced information for the vitreoretinal surgeon. (*Invest Ophthalmol Vis Sci.* 2011;52:3153–3159) DOI:10.1167/iovs.10-6720

From the <sup>1</sup>Duke Eye Center, Duke University Medical Center, Durham, North Carolina; the <sup>2</sup>Cole Eye Institute, Cleveland Clinic Foundation, Cleveland, Ohio; and the <sup>3</sup>Department of Biomedical Engineering, Duke University, Durham, North Carolina.

Supported in part by National Center for Research Resources (NCRR) Grant 1UL1 RR024128-01 and National Eye Institute Grant R21-EY-019411.

Submitted for publication October 14, 2010; revised December 6, 2010; accepted December 6, 2010.

Disclosure: J.P. Ehlers, None; Y.K. Tao, P; S. Farsiu, None; R. Maldonado, None; J.A. Izatt, Biopogen (I), P; C.A. Toth, Alcon (C), Genentech (C), P

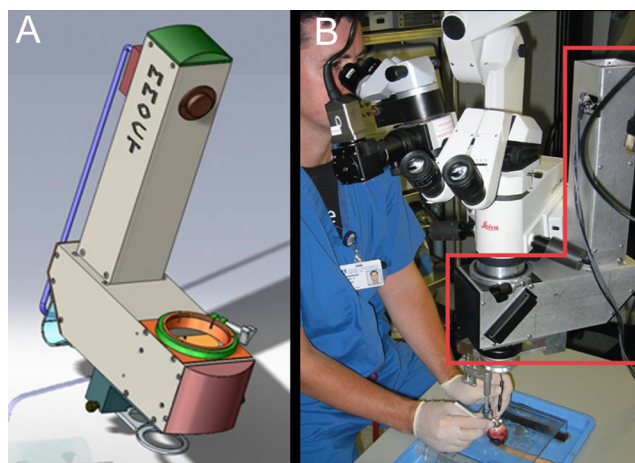
Corresponding author: Cynthia A. Toth, Box 3802, DUMC, Durham, NC 27710; cynthia.toth@duke.edu.

Over the years, multiple milestones have revolutionized vitreoretinal surgery. The *x-y* surgical microscope control, wide-angle viewing, and fiberoptic illumination are all examples of instrumentation that have been integrated to radically improve pars plana vitreoretinal surgery.<sup>1–6</sup> A major advance in vitreoretinal surgery may be the integration of retinal imaging into the operating room. Optical coherence tomography (OCT) has dramatically increased the efficacy of treatment of ophthalmic disease through improvement in diagnosis, understanding of pathophysiology, and monitoring of progression over time. Its ability to provide a high-resolution, cross-sectional, three-dimensional view of the relationships of vitreoretinal anatomy during surgery makes intraoperative OCT a logical complement to the vitreoretinal surgeon.

Early attempts at intraoperative OCT have already improved our understanding of the feasibility of intraoperative management and the role it might play in surgical decision-making. Epiretinal membrane (ERM) relationships, macular hole configurations, optic pit characteristics, retinal detachment features, and features of retinopathy of prematurity (ROP) have all been described by means of intraoperative OCT (Lee LB, et al. *IOVS* 2010;51:ARVO E-Abstract 6076).<sup>7–10</sup> One major limitation of intraoperative OCT is the availability of a device that integrates OCT capability into the operating microscope. Until now, published studies have used an OCT system separate from the operating microscope for imaging during surgery or for examination of patients under anesthesia.<sup>7–10</sup> When the current systems are used for intraoperative scanning, surgery must be halted while the scans are performed. Thus, one can image retinal architecture and vitreoretinal relationships after manipulations, but cannot obtain real-time OCT imaging of actual tissue manipulation.

The ideal device would provide a real-time platform for true intraoperative feedback to the surgeon. This approach would require device integration with the microscope, to allow for OCT scanning during surgery and should provide the surgeon with OCT visualization without interfering with the view of the real-time operative field. In addition, surgical instrumentation should be visible on OCT imaging while not obstructing the view of the underlying tissues.

In this study, we developed and tested a prototype microscope-mounted spectral domain (SD)OCT device to evaluate its potential for use in retinal microsurgery on the posterior pole. We also characterized the OCT appearance of the current armamentarium of instruments to better understand what is required for a fully integrated operative system, including the operative microscope, SDOCT, and OCT-compatible instrumentation.



**FIGURE 1.** (A) Illustration of the MMOCT prototype and (B) photograph of the operating microscope and MMOCT system (red box). Surgical manipulations are being performed on cadaveric porcine eye.

## METHODS

### Prototype Design

The microscope-mounted SDOCT system (MMOCT) was designed to be attached to an ophthalmic surgical microscope (model M841; Leica, Wetzlar, Germany) with an adapter for wide-field indirect ophthalmoscopy (BIOM3; Oculus, Wetzlar, Germany; Fig. 1A). The device is L-shaped. The horizontal housing is  $4 \times 4 \times 11.5$  inches, and the vertical housing is  $3 \times 3 \times 13$  inches. The wide-field adapter optically delivers an inverted wide-angle view of the retina to the image plane of the surgical microscope by the use of a high-power noncontact lens. When positioned adjacent to the objective lens of the surgical microscope, the adapter relays a large field-of-view image of the fundus to the viewport of the surgical microscope. The MMOCT imaging arm includes two-axis galvanometer mirrors to provide a raster-scanned image of the retina and a beam expander and relay optics to compensate for the large demagnification introduced by the view adapter, as a means of preserving lateral resolution. The SDOCT scanning beam was optically folded into the path of the surgical microscope by a dichroic mirror positioned between the microscope objective lens and the imaging optics of the viewports. The position of the dichroic-fold mirror was chosen to limit the physical size of the MMOCT attachment, to minimize the increase in the height of the scope (i.e., the distance from the surgical field to the surgeon's eyepieces). The MMOCT device increases the axial distance from the surgical oculars to the surgical field by 4 in. However, the oculars of the scope can be adjusted for the comfort of the surgeon.

The coatings on the dichroic mirror were custom made to avoid altering the view through the microscope, and the combined optical paths allowed for a common focus between the surgical microscope and the MMOCT view.<sup>11</sup> Custom software (Bioptigen, Durham, NC) was used to perform real-time data acquisition, processing, archiving, and display.

The device has been specifically designed to avoid interfering with the physical aspects of the surgery. However, if the device for some reason does interfere, there are various ways to correct the problem. If the device interferes from an optics standpoint, the dichroic mirror can be easily removed from the housing at any time. If this is removed from the housing, there are no changes in the optics that the surgeon utilizes from the native microscope. If the device physically interferes with the surgery, there is a collar clamp that mounts the MMOCT to the microscope that can be loosened manually. A securing bracket is removed with two screws, and the objective lens of the microscope is refastened to the bottom of the scope.

## Subjects

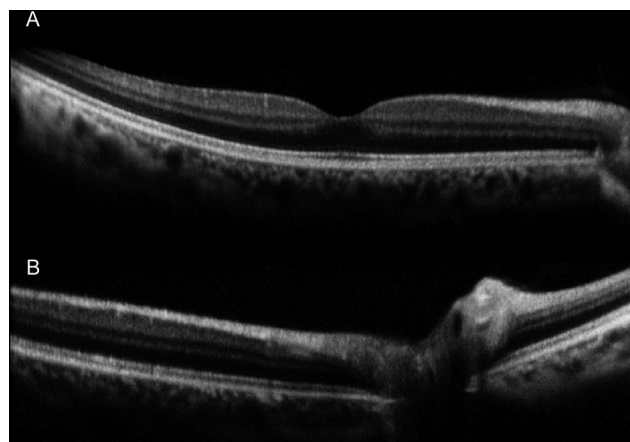
Intuitional Review Board approval was obtained, and all portions of the study were performed in compliance with the tenets of the Declaration of Helsinki. Healthy volunteers were recruited for imaging with the MMOCT device. The subject was positioned supine on a gurney, and the surgical microscope and MMOCT device were maneuvered over the subject for SDOCT scanning of the posterior pole.

## Model Eye Studies

Fresh cadaveric porcine eyes were obtained for imaging. To optimize corneal clarity and image quality, we performed OCT scanning within 12 hours of harvesting the eyes. Using a suction platform to fixate the eye, we positioned each eye under the surgical microscope and MMOCT (Fig. 1B). Two sclerotomies were created with a 19-gauge microvitrectomy (MVR) blade (Bausch and Lomb/Storz, Rochester, NY): one at the 2 o'clock position and one at the 10 o'clock position. A 20-gauge fiberoptic light was used for illumination, and the instrument of choice was maneuvered through the other sclerotomy. The wide-field adapter was used to adjust the focus for the surgeon and the OCT device. Volume scanning was performed before instrument manipulation and with each instrument in multiple locations superficial to the retina in the vitreous and on the retinal surface and while manipulating the retinal tissue (as appropriate for the instrument being imaged). Volumetric scans ( $15 \times 15$  mm) sampled at 500 A-scans with 2,048 spectral pixels per A-scan by 500 B-scans were obtained with the instrument maintained static at a specific position, at 20,000 A-scans per second. Alignment of the OCT scanning beam and the instrument was achieved by surgeon manipulation while viewing both the retinal surface and the live OCT scan.

## Instruments

Multiple instruments were used. They were chosen for their common use in vitreoretinal surgery, their composition, and their shape. Instruments tested included end-grasping metallic intraocular forceps (Alcon, Fort Worth, TX), a metallic subretinal needle (Alcon), a polyamide subretinal needle (Bausch and Lomb/Storz), a diamond-dusted membrane scraper (Synergetics, O'Fallon, MO), a silicone soft tip (Alcon), and a metallic MVR blade (Bausch and Lomb/Storz). The OCT characteristics of each instrument were evaluated, including visualization on the summed voxel projection (SVP),<sup>12</sup> visualization on the B-scan, reflectivity profile, shadowing of the tissue below the instrument, and visualization of tissue interaction.



**FIGURE 2.** MMOCT B-scan through the fovea (A) and the optic nerve (B) in eyes of health human volunteers.

## RESULTS

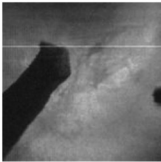
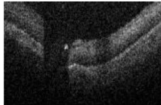
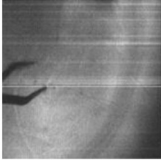
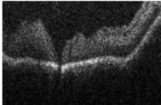
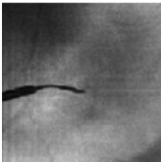

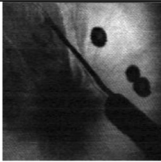
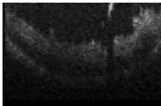
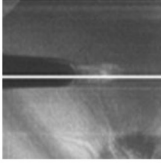
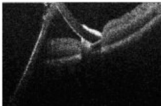
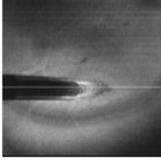
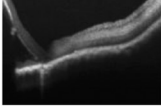
### In Vivo Human Imaging

In vivo human retinal SDOCT images were successfully acquired using the MMOCT system to view the posterior pole of four eyes of four volunteers. Images obtained were of similar structural resolution and quality as those obtained with current-generation SDOCT systems. Retinal architecture was well visualized, and scans of both the macula and optic nerve were obtained (Fig. 2).

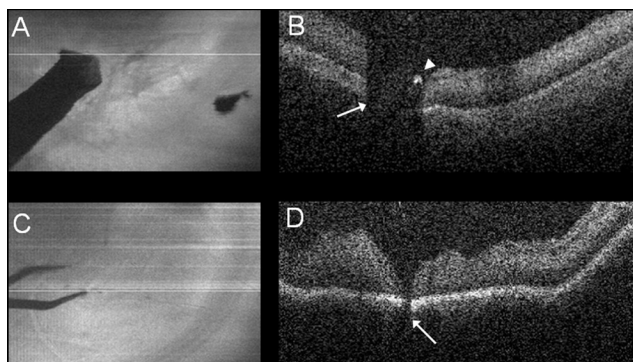
### Intraoperative Imaging and Instrument Visualization

In each case, high-quality images of the porcine retina were obtainable before surgical manipulation of the tissue. Each instrument was successfully imaged on the SVP. Each instrument had a unique reflectivity profile (Table 1). Metallic instruments showed absolute shadowing with bright reflectivity at the edge of the instrument. The low scattering properties of the metallic instruments limited the visualization of the instrument on the B-scan. Silicone and polyamide instruments had partial shadowing characteristics with partial visualization of

TABLE 1. OCT Characteristics of Intraocular Instruments

	Reflectivity	Shadowing	Visualized on Summed voxel projection (SVP)/B-scan	Surgical Manipulation Performed with Imaging	SVP Sample	B-scan Sample
MVR Blade	Very bright	Total	Yes/Limited	Engaging, scraping		
Metallic Forceps	Very bright	Total	Yes/Limited	Grasping retinal tissue and peripapillary glial tissue		
Metallic subretinal needle	Very bright	Total but limited significance because of small size of instrument	Yes/Yes	Subretinal space cannulation Creation of localized retinal detachment Retinal vein cannulation		
Polyamide subretinal needle	Bright	Significant but not absolute	Yes/Yes	Subretinal space cannulation		
Diamond-Dusted Membrane Scraper	Bright at diamonds, but moderate at silicone	Moderate, greater shadowing below diamonds.	Yes/Yes	Engaging retinal surface		
Silicone soft-tip	Moderate	Minimal	Yes/Yes	Engaging retinal surface		





**FIGURE 3.** MMOCT scans of surgical instruments. (A) MMOCT SVP image of an MVR blade. (B) MMOCT B-scan of the MVR blade shows total shadowing under the metallic instrument (*arrow*). The tip of the instrument is seen as a hyperreflective signal at the leading edge of the shadow (*arrowhead*). (C) MMOCT SVP of forceps resting on the retinal surface. (D) MMOCT B-scan with forceps resting on retinal surface. Near total shadowing is seen underneath the instrument tip (*arrow*). Compression of the retinal tissues is seen at the area of the tip.

the underlying tissues. Diamond dusting created a high reflectivity profile with increased shadowing compared with silicone. The high light-scattering properties of the nonmetallic instruments provided improved visualization of the instrument on the B-scan.

### Visualization of Intraoperative Maneuvers

Surgical manipulations with each instrument were successfully imaged in a static fashion. Maneuvers imaged with the MMOCT were as follows: manipulation of the retinal surface (e.g., MVR blade [Figs. 3A, 3B]; forceps [Figs. 3C, 3D]), grasping of tissue with forceps (e.g., retinal tissue or peripapillary glial tissue), engaging the retinal surface with a diamond-dusted membrane scraper and silicone soft-tip (Fig. 4), retinal vein cannulation with a subretinal needle (Fig. 5), and subretinal space cannulation with a subretinal needle. In addition to visualizing the planned operative maneuvers, intraoperative retinal effects were successfully imaged, including retinal contusion, retinal holes (Figs. 6A, 6B), retinal tears (Figs. 6C, 6D), disturbance of the retinal pigment epithelium, retinal traction, and creation of localized retinal detachment with a subretinal needle (Figs. 6E, 6F).

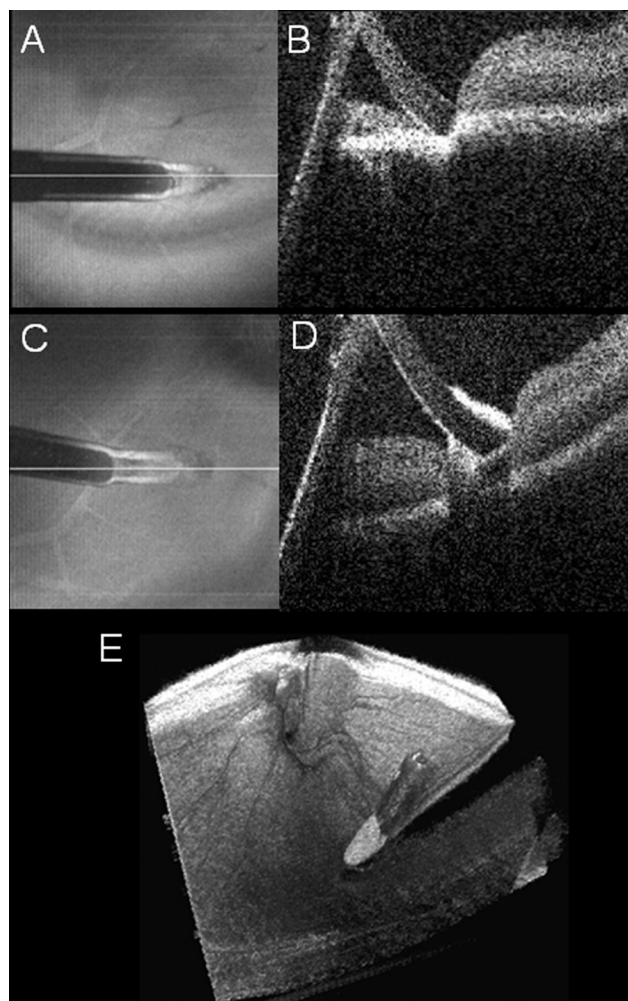
### Limiting Factors for Intraoperative Imaging

The challenges encountered during surgical maneuvers included time to align and capture SDOCT images, surgeon's display, vitreous interference, and different patterns of reflectivity of surgical instruments. For successful imaging of the area of interest, significant interaction was necessary between the operator of the MMOCT system and the surgeon, to localize the instrument. With the associated challenges of instrument localization, the surgeon was required to maintain a single position before manipulation while alignment was achieved. Once alignment was achieved, the surgeon had to maintain a static position while scanning was performed. This necessarily resulted in delays in performing the surgical maneuvers. Once aligned, the volumetric scan acquisition required 12.5 seconds with the scan protocol used—a volume scan with a sampling rate of 500 B-scans. Most commercial systems use a sampling rate of 125 to 200 B-scans per volume, which if used with the prototype would take less than half the time to acquire than did the 500 scans obtained in these pilot samples.

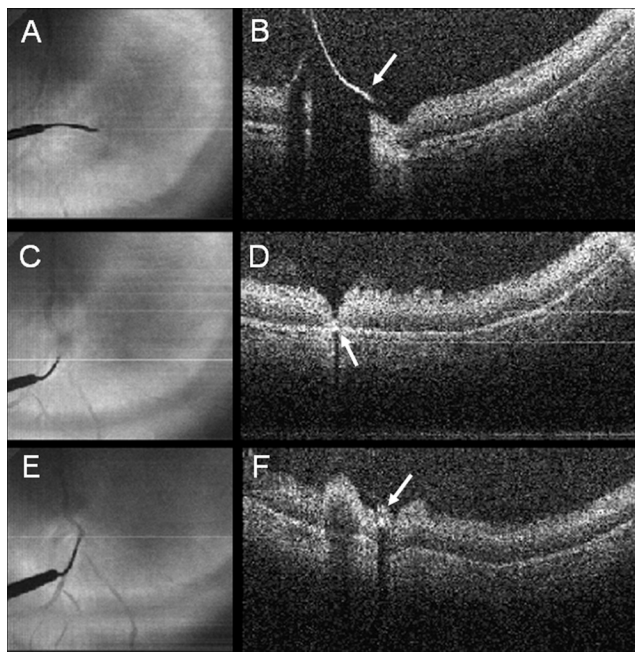
The overall quality of the model eye intraoperative OCT scans compared with the eyes of the human volunteers was lower. A major factor that contributed to the change in quality

was the use of cadaveric eyes. After death, the optical quality of the cornea and lens decreases slightly, and the retina rapidly becomes more opaque with loss of layers on OCT, resulting in an evenly hyperreflective retinal OCT image, as seen in the cadaveric porcine scans (personal communication C. Toth based on porcine studies in McCall et al.<sup>13</sup> and Choma MA, et al. *IOVS* 2002;43:ARVO E-Abstract 4372). It is unclear whether a similar change in quality would be appreciated when the scans are performed during surgical manipulations in vivo.

The separate OCT display system also created a disruption in the flow of surgery. The lack of a heads-up display system required the surgeon to look away from the operating microscope, resulting in a delay and preventing additional concurrent surgical maneuvers. To perform further surgical manipulations, the surgeon had to look away from the OCT display and return to the operating microscope view.



**FIGURE 4.** MMOCT scans of surgical instruments. (A) MMOCT SVP image of a silicone soft-tip. (B) MMOCT B-scan of silicone soft-tip on the retinal surface shows moderate reflectivity and minimal shadowing at tip. Total shadowing from the metallic handle is visible at the left of the image. (C) MMOCT SVP of diamond-dusted membrane scraper. (D) MMOCT B-scan of diamond-dusted membrane scraper on the retinal surface. Minimal shadowing and moderate reflectivity are caused by the posterior silicone-only portion of the tip. Increased shadowing and hyperreflectivity appear in the area of the diamond-dusted tip. (E) MMOCT 3-D reconstruction of the diamond-dusted membrane scraper with hyperreflectivity in the area of the diamond dust. The silicone portion appears to be moderately reflective. Total shadowing is noted posterior to the silicone portion, secondary to the instrument handle.



**FIGURE 5.** MM OCT scans of a metallic subretinal needle. MM OCT (A) SVP image and (B) B-scan of the subretinal needle above the retina before retinal vein cannulation. The subretinal needle is highly reflective (arrow), with total shadowing appearing beneath the needle tip. Retinal compression secondary to the vitreous is seen just in front of the needle. MM OCT (C) SVP and (D) B-scan of a subretinal needle (arrow) penetrating the subretinal space during attempted cannulation. Significant shadowing is seen below the needle. MM OCT (E) SVP and (F) B-scan of subretinal needle (arrow) successfully cannulating the retinal vein. Significant shadowing is noted below the needle.

The OCT characteristics of instrumentation also limited the amount of information obtained from the intraoperative scans. Total shadowing from metallic instruments eliminated views to the underlying tissues during manipulation. The shadowing and minimal scattering associated with the metallic instruments also limited views of the instruments on B-scan, although the SVPs captured the instruments nicely (Fig. 4). In addition to the shadowing, inversion of the captured B-scan occurred with the increased vertical height associated with the instrument within the area of the scan-limited interpretation of the acquired images in the area of inversion. This effect was also problematic during injection of subretinal fluid, as the retinal height exceeded the depth that could be captured on the B-scan.

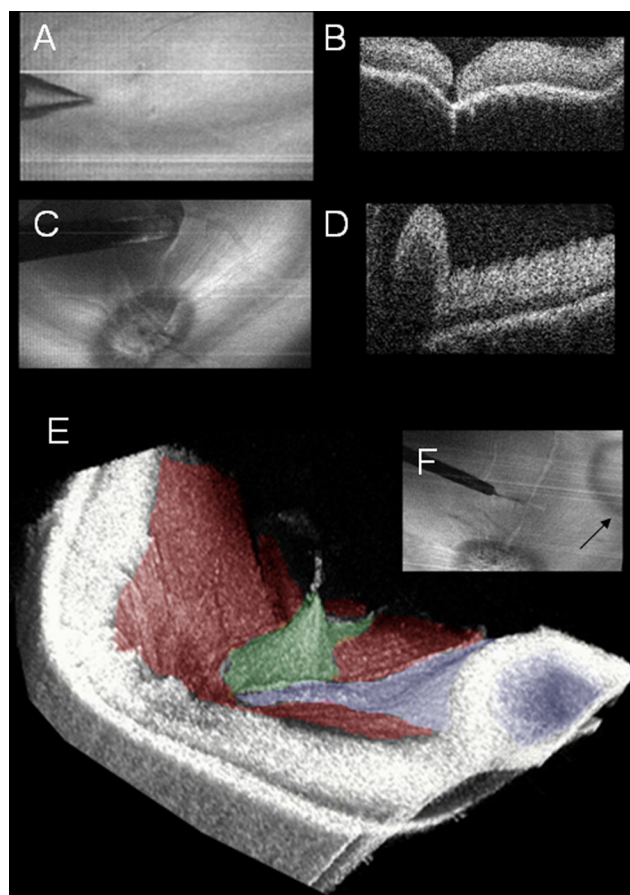
Finally, surgical manipulations were performed in nonvitrectomized eyes. The density of the porcine vitreous resulted in compression of the underlying tissue as the retina was approached with the various instruments. The compression of the underlying tissue changed the retinal architecture and relationship between the instrument and the retina. In addition, the density of the vitreous would inhibit free movement of the finer instruments (e.g., subretinal needle) through the vitreous cavity.

## DISCUSSION

In this study, we report the successful integration of an SDOCT system with the operating microscope head. Imaging of both human and the porcine retinas was feasible. In addition, multiple surgical instruments were imaged with MM OCT while a surgeon performed intraoperative maneuvers. In our review of the literature, we did not find any published reports regarding

MMSDOCT systems, the OCT characteristics of instrumentation, or OCT-based visualization of intraocular maneuvers. The prototype MM OCT device adds a 4-in. vertical increase to the axial distance from the surgical oculars and the surgical field. The extended-length oculars of the scope can be lowered to account for most of this height. For comfort, further modifications that lower the oculars may be useful for some surgeons using this system. Because the device is located above the objective lens and the wide-field viewing system of the microscope, it does not affect focusing. There were no difficulties related to the physical presence of the MM OCT device in performing the maneuvers or in focusing during the maneuvers.

Vitreoretinal surgery has made remarkable progress over the past few decades. Advances in surgical instrumentation, illumination, and vital dyes have all transformed the surgical landscape of the retina.<sup>3,5,14,15</sup> The intraoperative integration of SDOCT may be the next major step in vitreoretinal surgery. Early research suggests that intraoperative OCT may yield critical information regarding disease states, impact of surgical maneuvers, and intraoperative anatomic configurations.



**FIGURE 6.** MM OCT scans showing tissue effects from operative maneuvers. (A) MM OCT SVP image showing a retinal hole with forceps grasping tissue in another area. (B) MM OCT B-scan of full-thickness retinal hole after grasping of retinal tissue with metallic forceps. (C) MM OCT SVP of scrolled retina and retinal elevation after penetration of the retinal surface with the silicone-tipped instrument. (D) MM OCT B-scan of corresponding area with silicone tip embedded in retinal tissue. (E) MM OCT 3-D reconstruction of retinal traction (green) from subretinal needle after injection of subretinal fluid (blue). Red: attached retina. (F) MM OCT SVP of corresponding area with visualization of the subretinal needle and associated area of subretinal fluid (arrow).



Intraoperative OCT has been used to examine multiple vitreoretinal diseases including optic pit-related maculopathy, ROP, ERM, macular holes, and retinal detachment. It provides the opportunity to achieve a greater understanding of the pathophysiology of vitreoretinal surgical pathology. For example, intraoperative analysis of pars plana vitrectomy for optic pit maculopathy has suggested a connection between the vitreous cavity and the macular retinoschisis.<sup>10</sup> In addition, intraoperative OCT in ROP has revealed preretinal structures and retinoschisis that has not been identified clinically.<sup>7</sup>

In addition to providing information regarding pathophysiology, intraoperative OCT allows a surgeon to visualize the impact of a surgical maneuver on the tissues of interest. In macular holes, intraoperative OCT has demonstrated changes in hole configuration, successful removal of the internal limiting membrane, and visualization of retinal distortion and architecture changes related to surgical maneuvers (Ray JA, et al. *IOVS* 2010;51:ARVO E-Abstract 2962; Binder S, et al. *IOVS* 2010;51:ARVO E-abstract 268).<sup>8</sup> After ERM removal, intraoperative imaging has revealed rapid improvement in retinal architecture and subclinical neurosensory retinal detachment in some cases (Baranano AE, et al. *IOVS* 2010;51:ARVO E-Abstract 269).<sup>8</sup> Persistent subretinal fluid following perfluorocarbon liquid tamponade has been identified by intraoperative SDOCT in cases of macula-involving retinal detachment (Lee LB, et al. *IOVS* 2010;51:ARVO E-Abstract 6076). In addition to information on the maneuvers performed, intraoperative OCT may provide feedback that helps guide additional surgical maneuvers. One example is residual membranes that may not be appreciated clinically but could then be removed intraoperatively with OCT confirmation of removal (Baranano AE, et al. *IOVS* 2010;51:ARVO E-Abstract 269).<sup>9</sup>

Currently, there are no commercially available MMOCT units. A microscope-mounted prototype using the Cirrus (Carl Zeiss Meditec, Oberkochen) system has been presented, but to our knowledge, no reports have been published (Binder S, et al. *IOVS* 2010;51:ARVO E-abstract 268). Because of the lack of MMOCT systems, visualizing instrumentation and direct tissue manipulations with intraoperative OCT has not been possible. Using the MMOCT system, we described the wide-ranging OCT characteristics of intraocular instruments. Metallic instruments exhibited very high reflectivity with total shadowing. These characteristics make metallic instruments less than ideal for intraoperative manipulations while using OCT. Visualization of the underlying tissue and interfaces between instrumentation and tissues was limited. On the other hand, nonmetallic instruments (e.g., silicone, polyamide) provided improved visualization of the underlying tissues and the interactions between the instrument and the retinal surface. As OCT becomes more integrated into the operating room, new instrumentation with improved reflectivity profiles may have to be designed. For example, the current metallic forceps would limit OCT visualization of real-time membrane peeling due to severe shadowing. On the other hand, polyamide or PMMA-tipped forceps might allow real-time OCT visualization of intraocular maneuvers and instrument-tissue interactions.

An alternative to changing instrument materials to improve visualization may include real-time image processing of the intraoperative scans. Since the position of the surgical instrument would not necessarily remain constant over the several milliseconds required between sequential depth cross-sectional acquisitions, multiple spatially correlated B-scans may be co-registered and either stitched, mosaicked, or averaged to fill in any tissue regions obscured by instrument shadowing (Estrada R, et al. *IOVS* 2010;51:ARVO E-abstract 5928). These image-processing techniques take advantage of the fact that any motion of the instrument by the surgeon would be much larger than the lateral thickness of each depth cross-section;

thus, shadowed regions of the tissue are decorrelated and can therefore be filled in rapidly by image processing. While potentially useful for removing shadowing artifacts, these techniques require real-time, high-resolution tracking and registration algorithms that may increase the computational cost of current data acquisition and visualization software.

A major limitation in intraoperative scanning of procedures is the efficient targeting of the OCT scan to the area of interest. The cross-sectional nature of B-scan OCT images necessitates precise targeting of the OCT device. Because of the dynamic nature of intraocular maneuvers, rapid targeting of the OCT scan is critical for the device to be fully integrated into surgical decision-making. There are multiple approaches to consider in facilitating scan targeting. One possibility is direct instrument modifications. One published report of instrument modifications includes direct integration of the OCT imaging fiber into the device.<sup>16</sup> Although this approach would provide direct localization of the OCT scan, it may limit image quality due to instrument size and may limit the surgeon to using intraoperative OCT with only those instruments that have the built-in system. An alternative would be to create a dynamic aiming system with the tip of the instrument serving as a tracer for the OCT laser. This method would allow for rapid imaging at the tip of the instrument and for use of an MMOCT system. Finally, custom real-time image analysis may also help in guiding the SDOCT scanner to the area of interest. Various frameworks and algorithms have been described for tracking position and changes in scene during image processing.<sup>17-19</sup> These processing algorithms may be used to help guide the location of the scanning beam to the location of the instrument and intraoperative maneuvers.

Current display systems for OCT imaging are also a limiting factor for its widespread use in the operating room. Currently, images are displayed on a monitor, causing the surgeon to look away from the microscope. When imaging intraoperatively after a surgical maneuver, this limitation is not problematic. However, for real-time visualization of surgical maneuvers, having the surgeon look away from the microscope may risk patient safety. This problem limits the feedback that the surgeon can receive from the real-time scan. Heads-up display systems have widespread use in automobiles and aviation. These displays reduce risk to the driver or pilot by allowing them to maintain a field of view in the environment while providing feedback of information, such as speed or altitude. In addition, in neurosurgery the use of heads-up displays has been adapted to surgical microscopes for integration of imaging information with real-time stereotactic surgery.<sup>20</sup> A similar system could be used in the vitreoretinal operating room to allow for a heads-up display that enables simultaneous viewing of the real-time OCT images and the operative field. Such a display would provide the surgeon with rapid feedback of intraocular maneuvers through both OCT information and direct visualization. A critical component of this system would be the presentation of critical intraoperative data rather than the entire data set. Using a subset of the information that is critical for maneuvers would help to avoid information overload for the surgeon and reduce the potential distraction that too much information might provide.

Future applications of integrated MMOCT could include both quantitative and qualitative depth and tissue proximity information to the surgeon. The cross-sectional nature of the B-scan would allow for a qualitative display for the surgeon to view, to determine the proximity of the instrumentation to the tissue of interest. In addition, the use of automated segmentation algorithms may allow for real-time quantitative measurements of proximity of the surgical instrument to the retinal layers of interest.<sup>21</sup> This real-time information could be inte-

grated into the surgical procedure in various ways, including audio-based proximity alarms and measurement guide displays.

In this study, we report the successful integration of MMOCT into the surgical microscope. The platform was able to be used to image human volunteers as well as multiple instruments and surgical maneuvers in porcine eyes. The feedback from the system allowed visualization of instrument-tissue interactions during surgical maneuvers. The development of MMOCT is a major step toward integration of OCT in the vitreoretinal surgical environment. Further study of instrumentation design, OCT scanning protocols, means of capturing intraoperative motion, instrument tracking, display technology, image processing, and real-time intraoperative imaging in human subjects is needed.

## References

1. Machemer R, Buettner H, Norton EW, Parel JM. Vitrectomy: a pars plana approach. *Trans Am Acad Ophthalmol Otolaryngol*. 1971; 75:813-820.
2. Machemer R, Buettner H, Parel JM. Vitrectomy, a pars plana approach: instrumentation. *Mod Probl Ophthalmol*. 1972;10:172-177.
3. Machemer R, Parel JM. An improved microsurgical ceiling-mounted unit and automated television. *Am J Ophthalmol*. 1978; 85:205-209.
4. Parel JM, Machemer R, Aumayr W. A new concept for vitreous surgery, 5: an automated operating microscope. *Am J Ophthalmol*. 1974;77:161-168.
5. Parel JM, Machemer R, Aumayr W. A new concept for vitreous surgery, 4: improvements in instrumentation and illumination. *Am J Ophthalmol*. 1974;77:6-12.
6. Spitznas M. A binocular indirect ophthalmomicroscope (BIOM) for non-contact wide-angle vitreous surgery. *Graefes Arch Clin Exp Ophthalmol*. 1987;225:13-15.
7. Chavala SH, Farsiu S, Maldonado R, Wallace DK, Freedman SF, Toth CA. Insights into advanced retinopathy of prematurity using handheld spectral domain optical coherence tomography imaging. *Ophthalmology*. 2009;116:2448-2456.
8. Dayani PN, Maldonado R, Farsiu S, Toth CA. Intraoperative use of handheld spectral domain optical coherence tomography imaging in macular surgery. *Retina*. 2009;29:1457-1468.
9. Scott AW, Farsiu S, Enyedi LB, Wallace DK, Toth CA. Imaging the infant retina with a hand-held spectral-domain optical coherence tomography device. *Am J Ophthalmol*. 2009;147:364-373-e2.
10. Ehlers J, Kernstine K, Farsiu S, Sarin N, Maldonado R, Toth C. Real-time analysis of pars plana vitrectomy for optic pit-related maculopathy with intraoperative spectral domain optical coherence tomography: a connection with the vitreous cavity. *Arch Ophthalmol*. In press.
11. Tao Y, Ehlers J, Toth C, Izatt J. Intraoperative spectral domain optical coherence tomography for vitreoretinal surgery. *Opt Lett*. 2010;35:3315-3317.
12. Jiao S, Knighton R, Huang X, Gregori G, Puliafito C. Simultaneous acquisition of sectional and fundus ophthalmic images with spectral-domain optical coherence tomography. *Opt Express*. 2005;13: 444-452.
13. McCall M, Harkrider CJ, Deramo V, et al. Using optical coherence tomography to elucidate the impact of fixation on retinal laser pathology: Laser-Tissue Interaction XII: Photochemical, Photothermal, and Photomechanical. *SPIE Proc* 2001;4257:142-148.
14. Kadonosono K, Itoh N, Uchio E, Nakamura S, Ohno S. Staining of internal limiting membrane in macular hole surgery. *Arch Ophthalmol*. 2000;118:1116-1118.
15. Machemer R, Parel JM, Hickingbotham D, Nose I. Membrane peeler cutter: automated vitreous scissors and hooked needle. *Arch Ophthalmol*. 1981;99:152-153.
16. Balicki M, Han JH, Iordachita I, et al. Single fiber optical coherence tomography microsurgical instruments for computer and robot-assisted retinal surgery. *Med Image Comput Comput Assist Interv*. 2009;12:108-115.
17. Lelescu D, Schonfeld D. Statistical sequential analysis for real-time video scene change detection on compressed multimedia bitstream. *IEEE Trans*. 2003;5:106-117.
18. Peterfreund N. Robust tracking of position and velocity with Kalman snakes. *IEEE Trans Pattern Anal Mach Intell*. 1999;21:564-569.
19. Ulrich M, Steger C, Baumgartner A. Real-time object recognition using a modified generalized Hough transform. *Pattern Recogn*. 2003;36:2557-2570.
20. Nimsy C, Ganslandt O, Fahlbusch R. Implementation of fiber tract navigation. *Neurosurgery*. 2007;61:306-317, discussion 317-318.
21. Chiu S, Li X, Nicholas P, Toth C, Izatt J, Farsiu S. Automatic segmentation of seven retinal layers in SDOCT images congruent with expert manual segmentation. *Opt Express*. 2010;18:19413-19428.